A Deep-Learning Based Framework for Joint Downlink Precoding and CSI Sparsification

Jianjun Zhang, Christos Masouros, XXX, XXX

Department of Electronic & Electrical Engineering, University College London, London WC1E7JE, U.K.
Email: {jianjun.zhang,c.masouros}@ucl.ac.uk

***Abstract*—Optimal pilot design to acquire channel state information (CSI) is of critical importance for FDD downlink massive MIMO systems, and is still an open problem. To tackle this issue, in this paper we propose a two-stage precoding approach based on reduced CSI (rCSI-TSP) design framework and an efficient algorithm, whose core is to obtain an optimal precoder while also sparsifying physical CSI (pCSI), so as to save on CSI estimation. The advantages of the framework are three-fold. First, the framework enables to simultaneously extract and exploit statistical and instantaneous CSI. Second, it guarantees the most needed rCSI can be obtained and thus avoids performance loss due to heuristic pilot design. Third, we tailor an efficient online deep-learning based method for the TSP framework, which paves the way for practical applications. As an example, we apply the framework to the multi-user symbol-level precoding (SLP) and verify performance improvements.**

***Index Terms*—Task-oriented pilot design, perception and reasoning, rCSI precoding, intelligent wireless communication.**

I. Introduction

The high spectrum and energy efficiency and tolerance to simple signal processing techniques have established massive multiple-input multiple-output (MIMO) as a key 5G technology [1]. To reap the benefits of massive MIMO, CSI between transceivers is indispensable. However, due to the prohibitively high overhead associated with downlink training and uplink feedback, the acquisition of downlink CSI is recognized as a very challenging task for massive MIMO systems. This is particularly pronounced for the FDD massive MIMO systems, where the channel reciprocity between the uplink channels and downlink counterparts cannot be exploited [1].

As an effective means to improve the system performance, precoding has always been an active research area [2], [3]. In classical approaches, interferences are often regarded as a limitation and are suppressed as much as possible. However, seen from an instantaneous point of view, interferences can be constructive and can further be exploited through symbol-level precoding (SLP) [4]–[6]. In particular, the concept of constructive interference (CI) was exploited to improve system performance in [6]. As the first work on optimization based CI precoding, a low-complexity vector precoding scheme was proposed in [7] for multi-user downlink systems.

Because of the high dimension of channels in FDD massive MIMO systems, two-stage precoding (TSP) design paradigm has been widely investigated [3], [8]–[13]. In general, the first-stage precoding is introduced to adapt to channel statistics, while the second-stage precoding is utilized to improve system performance (e.g., to mitigate interference or achieve spatial multiplexing gain). The existing TSP works fall into two categories. In the first one, the two-stage precoders are designed to achieve the above goals, however, under the assumption that complete pCSI is available. Typically, the MIMO precoder at the base station is partitioned into a radio frequency (RF) precoder and a baseband precoder [9]. In particular, the RF precoder is adaptive to slow time-scale channel statistics to achieve array gains, and the baseband precoder is adaptive to fast time-scale low dimensional effective channel to achieve spatial multiplexing gains. It should be noted that the task of estimating pCSI is very challenging in the FDD massive MIMO systems. Therefore, it is desired to achieve the above goals without requiring estimating pCSI in practice.

To tackle the issue of challenging CSI estimation, joint CSI acquisition and precoding optimization design approach has beep widely studied, which constitutes the second category. For this category, channel statistics (e.g., channel correlation matrix) is utilized to alleviate the burden of CSI estimation. Typically, eigenvectors of the channel correlation matrix are used as FDD training pilot to obtain effective/equivalent CSI, based on which the second-stage precoder is optimized [3], [8]. Note, however, that on the one hand, it is nontrivial to estimate the channel correlation matrix in practice, and on the other hand, such a method is heuristic and no optimality is guaranteed, because, from the view of second-stage precoding design, the obtained effective CSI may not be the most needed or effective. In fact, optimal training pilot design for the FDD downlink system is still an open and difficult problem.

Thanks to the fast development of machine learning (ML), ML methods have permeated into wireless communications and promoted learning-based CSI acquisition or precoding designs. In terms of precoding, a deep neural network (DNN) is typically trained to approximate an optimization-based algorithm, under the assumption that CSI is available [14]. To achieve joint processing gains (e.g., to reduce both training and feedback overheads), core operations, including channel estimation, quantization, feedback and multi-user downlink precoding, are all represented by DNNs and trained in the end-to-end manner recently [15]. However, the end-to-end based training requires a huge number of samples, and the learned model via offline training can be easily outdated.

To address all aforementioned issues, in this paper we

propose a rCSI based two-stage precoding design framework and an efficient algorithm, aiming at saving on CSI estimation by making pCSI sparse. In particular, the rCSI-TSP framework incorporates perception and reasoning modules and functions. Specifically, the perception module (PM), implemented via a usual DNN, is designed to online sense and extract channel statistics. As a result, the pCSI is not required or provided, when compared to the first category (e.g., [9]). To guarantee that the estimated rCSI is the most needed by the second-stage precoder, we design elaborately the reasoning module (RM) via algorithm unrolling (AU), i.e., to unfold a precoding algorithm of interest and then append the unfolded network (referred to as reasoning network) to the PM network. The use of AU also greatly reduces the computational complexity of precoding [16]. We tailor a data-driven and online learning method to efficiently train the integrated network, so as to achieve our gaols (e.g., to extract channel statistics). We verify above advantages by applying these techniques to the FDD downlink multi-user SLP via comprehensive simulations.

II. System Model

Consider an FDD downlink multi-user communication system, which consists of a BS equipped with $N(\gg 1)$ transmit antennas and U single-antenna users (UEs). The set of U UEs is denoted by $\mathcal{U} = \{1, \cdots, U\}$. The channel vector between the BS and each UE $u \in \mathcal{U}$ is represented by $\bar{\mathbf{h}}_u \in \mathbb{C}^{N\times 1}$ with $\bar{\mathbf{h}}_u \sim \mathcal{CN}(\mathbf{0}, \mathbf{R}_u)$, where $\mathbf{R}_u = \mathbb{E}\{\bar{\mathbf{h}}_u \bar{\mathbf{h}}_u^{\mathrm{H}}\}$ is a positive semi-definite covariance matrix [17]–[19]. Note that $\mathbf{R}_u$ describes (transmit-side) spatial correlation, typically, caused by limited antenna spacing, insufficient scattering environment and so on, which widely exist in large-scale antenna systems.

Without loss of generality, PSK modulation scheme (with constellation $\mathcal{D}_u$ of size K_u for UE u) is considered in this paper. Let $s_u = e^{j\xi_u} \in \mathcal{D}_u$ be the intended PSK information symbol for UE u (with ξ_u the argument of s_u) and $\mathbf{x}$ be the transmitted signal. The signal received at UE u is given by

$$y_u = \bar{\mathbf{h}}_u^{\mathrm{H}} \mathbf{x} + n_u, \tag{1}$$

where $n_u \sim \mathcal{CN}(0, \sigma_{\mathrm{N}}^2)$ denotes random noise.

To improve energy efficiency, the idea of CI is exploited. For the PSK modulation, the key of the CI design principle can be captured by the following constraint ($\forall\, u \in \mathcal{U}$) [20]

$$\left|\mathrm{Im}(\bar{\mathbf{h}}_u^{\mathrm{H}} \mathbf{x} e^{-j\xi_u})\right| \le \left(\mathrm{Re}(\bar{\mathbf{h}}_u^{\mathrm{H}} \mathbf{x} e^{-j\xi_u}) - \gamma_u\right) \tan(\pi/K_u), \tag{2}$$

where, as an SNR metric, γ_u measures the quality of received signal of UE u. The above constraints enforce that the CI pushes received signals away from decision boundaries of the PSK constellation, therefore improving the received SNR without the need to increase the transmit power [20]. In this paper, we consider the power-minimization SLP problem, which can be formulated as [20]

$$\begin{aligned} \min_{\mathbf{x}} \quad & \|\mathbf{x}\|^2 \\ \text{s.t.} \quad & \left|\mathrm{Im}(\bar{\mathbf{h}}_u^{\mathrm{H}} \mathbf{x} e^{-j\xi_u})\right| \le \left(\mathrm{Re}(\bar{\mathbf{h}}_u^{\mathrm{H}} \mathbf{x} e^{-j\xi_u}) - \gamma_u\right) \cdot \\ & \qquad \tan(\pi/K_u),\ (\forall\, u \in \mathcal{U}). \end{aligned} \tag{3}$$

Since problem (3) is, in fact, a quadratic programming [7], it can be efficiently solved via convex optimization tools, if the pCSI $\{\bar{\mathbf{h}}_u\}$ is available. However, in practice it is difficult to obtain highly-precise pCSI, especially for FDD downlink multi-user systems. The reason is that the downlink CSI of an FDD system is obtained conventionally via downlink training and uplink feedback. However, overheads of both downlink training and uplink feedback are prohibitively high for a large-scale antenna system. Next, we propose an efficient algorithm to address these issues via the rCSI-TSP framework.

III. Modified CSI based Pilot and Precoding Design

We employ rCSI based unified pilot and precoding design technique [21] to alleviate the burden of CSI acquisition and feedback. For this purpose, we require the following lemma.

Lemma 1. *Let* $\mathbf{F}$ *be a matrix such that the set of all column vectors of* $\mathbf{F}$*, denoted by* $\mathcal{F}$*, spans vector space* $\mathbb{C}^N$*. Then, problem* (3) *is equivalent to the following problem*

$$\begin{aligned} \min_{\mathbf{v}} \quad & \|\mathbf{F}\mathbf{v}\|^2 \\ \textit{s.t.} \quad & \left|\mathrm{Im}(\bar{\mathbf{h}}_u^{H} \mathbf{F}\mathbf{v} e^{-j\xi_u})\right| \le \left(\mathrm{Re}(\bar{\mathbf{h}}_u^{H} \mathbf{F}\mathbf{v} e^{-j\xi_u}) - \gamma_u\right) \cdot \\ & \qquad \tan(\pi/K_u),\ (\forall\, u \in \mathcal{U}). \end{aligned} \tag{4}$$

Due to space limitation, it is referred to [21] for the proof. Lemma 1 indicates that to solve problem (3), it is sufficient to solve problem (4). Compared to problem (3), the advantage of problem (4) is that there is no need to estimate the original pCSI $\{\bar{\mathbf{h}}_u\}$. Instead, if modified CSI (mCSI), defined as $\{\mathbf{h}_u = \mathbf{F}^{\mathrm{H}} \bar{\mathbf{h}}_u\}$, is available, we can still obtain the optimal precoder. More importantly, by elaborately designing $\mathbf{F}$, the acquisition and feedback of mCSI $\{\mathbf{h}_u\}$ may be much easier. Typically, via appropriate design, $\{\mathbf{h}_u\}$ may be sparse, and thus training- and feedback-efficient. Based on Lemma 1, problem (4) can be reformulated as

$$\begin{aligned} \min_{\mathbf{v}} \quad & \|\mathbf{F}\mathbf{v}\|^2 \\ \text{s.t.} \quad & \left|\mathrm{Im}(\mathbf{h}_u^{\mathrm{H}} \mathbf{v} e^{-j\xi_u})\right| \le \left(\mathrm{Re}(\mathbf{h}_u^{\mathrm{H}} \mathbf{v} e^{-j\xi_u}) - \gamma_u\right) \cdot \\ & \qquad \tan(\pi/K_u),\ (\forall\, u \in \mathcal{U}). \end{aligned} \tag{5}$$

In practice, $\{\mathbf{h}_u\}$ should be replaced by the estimates $\{\hat{\mathbf{h}}_u\}$.

By regarding each element of $\mathcal{F}$ as a pilot beam, $\{\mathbf{h}_u\}$ can be estimated, based on which problem (5) can be solved. It is hoped that $\{\mathbf{h}_u\}$ can be sparse, since in this case it is sufficient to use an appropriate subset of $\mathcal{F}$ to estimate only important elements of each $\mathbf{h}_u$. The subset of $\mathcal{F}$ (or sub-matrix of $\mathbf{F}$) is still denoted by $\mathcal{F}$ (or $\mathbf{F}$). Note that a heuristic $\mathcal{F}$ is often not optimal, because an optimal $\mathcal{F}$ depends on $\{\bar{\mathbf{h}}_u\}$ and has to sufficiently match and adapt to environments. To efficiently acquire $\{\mathbf{h}_u\}$ with a much reduced CSI (rCSI) compared to the physical CSI (pCSI), $\mathbf{F}$ should also be optimized, i.e.,

$$\begin{aligned} \min_{\mathbf{F},\mathbf{v}} \quad & \|\mathbf{F}\mathbf{v}\|^2 \\ \text{s.t.} \quad & \left|\mathrm{Im}(\bar{\mathbf{h}}_u^{\mathrm{H}} \mathbf{F}\mathbf{v} e^{-j\xi_u})\right| \le \left(\mathrm{Re}(\bar{\mathbf{h}}_u^{\mathrm{H}} \mathbf{F}\mathbf{v} e^{-j\xi_u}) - \gamma_u\right) \cdot \\ & \qquad \tan(\pi/K_u),\ (\forall\, u \in \mathcal{U}). \end{aligned} \tag{6}$$

However, it is difficult to optimize $\mathbf{F}$ and $\mathbf{v}$ simultaneously, due to the coupling between $\mathbf{F}$ and $\mathbf{v}$ and high computational complexity. More difficultly, solving problem (6) requires the pCSI $\{\bar{\mathbf{h}}_u\}$, which forms a deadlock or endless loop.

To sufficiently exploit statistical and instantaneous CSI and meanwhile address the first difficulty, we propose our first idea. Specifically, we distinguish time-scales of optimizing $\mathbf{F}$ and $\mathbf{v}$, i.e., they are not optimized simultaneously. The key is to incorporate statistical and instantaneous information wisely and efficiently. The proposed method is as follows:

- $\mathbf{F}$ is designed to capture and extract channel statistical characteristics (in particular, spatial correlation information). The time-scale of optimizing $\mathbf{F}$ is large, e.g., it is updated every K channel coherence intervals (CCIs).
- The mCSI $\{\mathbf{h}_u\}$ captures instantaneous channel characteristics. The time-scale of estimating $\{\mathbf{h}_u\}$ is relatively small, i.e., it is estimated every CCI.

For clarity, the time-scales of optimizing $\mathbf{F}$ and updating mCSI $\{\mathbf{h}_u\}$ are illustrated in Fig. 1. There is no need to optimize $\mathbf{F}$ when estimating $\{\mathbf{h}_u\}$ and optimizing $\mathbf{v}$ (via solving problem (5)), by distinguishing the time-scales.

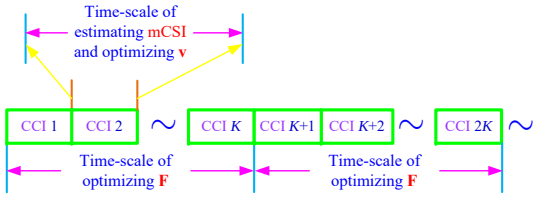

Fig. 1. Time-scales of optimizing $\mathbf{F}$ and estimating $\{\mathbf{h}_u\}$: mCSI $\{\mathbf{h}_u\}$ is estimated every CCI, while $\mathbf{F}$ is updated every K CCIs.

Next, we proceed to tackle the issue of optimizing/updating $\mathbf{F}$, so as to guarantee that the optimized $\mathbf{F}$ is task-oriented, i.e., it can sense the most needed mCSI. An obvious method is to represent the task (i.e., the precoding algorithm) by a DNN and train it end-to-end [15]. However, the obtained network is sample- or data-hungry and can be easily outdated, making this method impractical in practical environments. To avoid wasting precious samples/data on training the precoding DNN, we employ a convectional iterative algorithm to optimize the precoder $\mathbf{v}$. However, an optimization solver only provides a vector $\mathbf{v}$ for a given realization $\{\mathbf{F}^{\mathrm{H}}\bar{\mathbf{h}}_u\}$. Due to very limited information provided by $\mathbf{v}$, it is difficult to update $\mathbf{F}$.

Remark 3.1 We emphasize that this difficulty does not exist in a complete NN based algorithm (e.g., [15]). For an NN based algorithm, the structure and all mathematical operations (e.g., linear transforms and subsequent element-wise nonlinear operations) are deterministic. Hence, all information required to update the NN (e.g., gradients) can be obtained easily.

To address the above issue, we propose a joint perception and reasoning (JPR) framework, as shown in Fig.2. The design methodology and individual roles of the perception module (PM) and reasoning module (RM) are as follows:

- The PM is introduced and designed to sense the channel environment and extract channel statistical information. It is implemented via a usual DNN. The motivation is that DNN-based ML methods can automatically discover meaningful patterns from data. For the considered problem, it is in charge of representing/processing $\mathbf{F}$.
- The RM is stacked on top of the PM and is treated as an additional layer of the overall deep architecture. Note that the RM (i.e., reasoning network) is implemented by unfolding an iterative optimization-based algorithm. For the considered problem, the RM is mainly responsible for optimizing the precoder $\mathbf{v}$, given simultaneous mCSI.

Although the end-to-end training method can be used to train a JPR network, it cannot take maximum advantage of the JPR framework. To bring its superiority into full play, a tailored online learning method will be proposed later.

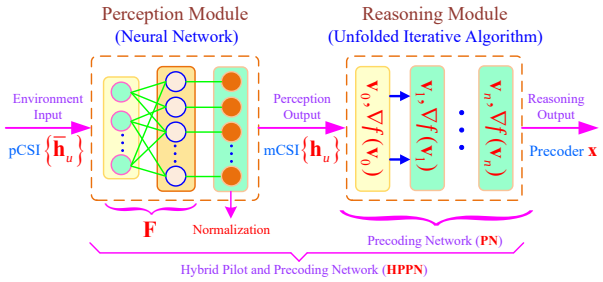

Fig. 2. An illustration of the joint perception and reasoning architecture.

Remark 3.2 Due to the stacked structure, information (e.g., gradients of the RM) required to update $\mathbf{F}$ can be efficiently propagated from the RM to the PM layer by layer. Note that because the AU technique is utilized to construct the reasoning network, both domain knowledge and model information can be retained, which, in contrast to the DNN-based implementation, greatly reduces the number of required samples.

IV. Intelligent Pilot Design via Joint Perception and Reasoning

In this section, we first employ the JPR technique to design an efficient precoding network, and then propose an efficient training method. Because of the linear form between pCSI and pilot matrix $\mathbf{F}$, the PM is designed as follows:

- The PM is implemented via a NN with three layers, i.e., an input layer, a hidden layer and a normalization layer. The weights between the input layer and the i-th hidden neuron is denoted by $\mathbf{f}_i$, i.e., the i-th column of $\mathbf{F}$.
- The size of the input layer is equal to the size of the antenna array, and the size of the hidden layer is equal to the number of pilot budget.
- In view that transmit pilot beams are often normalized to 1, the normalization layer is introduced. The mapping between the i-th hidden unit and the i-th output unit, i.e., $\mathbf{f}_i/\|\mathbf{f}_i\|$, can be regarded as an activation function.

It is important to introduce the normalization layer, since it limits the dynamic range of mCSI, which simplifies quantization design, e.g., the uniform scalar quantization works well.

A. Reasoning Module Design

Since the RM is implemented via AU [16], the first step is to design an iterative algorithm that can efficiently solve problem (5). Next, we employ the dual ascent approach to address this issue. Before presenting details, we first transform problem (5) with complex variable into a problem with real variables.

Let $\mathbf{v} = \mathbf{v}_{\mathrm{R}} + j\mathbf{v}_{\mathrm{I}}$ and $e^{j\xi_u}\hat{\mathbf{h}}_u = \tilde{\mathbf{h}}_{\mathrm{R},u} + j\tilde{\mathbf{h}}_{\mathrm{I},u}$, where $\mathbf{v}_{\mathrm{R}}$ and $\mathbf{v}_{\mathrm{I}}$ represent the real part and imaginary part of complex variable $\mathbf{v}$. The real vectors $\tilde{\mathbf{h}}_{\mathrm{R},u}$ and $\tilde{\mathbf{h}}_{\mathrm{I},u}$ are defined similarly. Then, problem (5) can be equivalently written as

$$\begin{aligned}\min_{\mathbf{v}_{\mathrm{R}},\mathbf{v}_{\mathrm{I}}}\ & \left(\mathbf{v}_{\mathrm{R}}^{\mathrm{T}}\mathbf{Q}_{\mathrm{R}}\mathbf{v}_{\mathrm{R}} + \mathbf{v}_{\mathrm{I}}^{\mathrm{T}}\mathbf{Q}_{\mathrm{R}}\mathbf{v}_{\mathrm{I}} - \mathbf{v}_{\mathrm{R}}^{\mathrm{T}}\mathbf{Q}_{\mathrm{I}}\mathbf{v}_{\mathrm{I}} + \mathbf{v}_{\mathrm{I}}^{\mathrm{T}}\mathbf{Q}_{\mathrm{I}}\mathbf{v}_{\mathrm{R}}\right)/2 \\ \text{s.t.}\ & \begin{bmatrix} C_u\tilde{\mathbf{h}}_{\mathrm{R},u}^{\mathrm{T}} + \tilde{\mathbf{h}}_{\mathrm{I},u}^{\mathrm{T}}, & C_u\tilde{\mathbf{h}}_{\mathrm{I},u}^{\mathrm{T}} - \tilde{\mathbf{h}}_{\mathrm{R},u}^{\mathrm{T}} \\ C_u\tilde{\mathbf{h}}_{\mathrm{R},u}^{\mathrm{T}} - \tilde{\mathbf{h}}_{\mathrm{I},u}^{\mathrm{T}}, & C_u\tilde{\mathbf{h}}_{\mathrm{I},u}^{\mathrm{T}} + \tilde{\mathbf{h}}_{\mathrm{R},u}^{\mathrm{T}} \end{bmatrix} \begin{bmatrix}\mathbf{v}_{\mathrm{R}} \\ \mathbf{v}_{\mathrm{I}}\end{bmatrix} \succeq \begin{bmatrix}\gamma_u \\ \gamma_u\end{bmatrix}, \quad (7) \\ & (\forall\, u \in \mathcal{U}),\end{aligned}$$

where $\mathbf{Q}_{\mathrm{R}} = \mathrm{Re}(\mathbf{F}^{\mathrm{H}}\mathbf{F})$, $\mathbf{Q}_{\mathrm{I}} = \mathrm{Im}(\mathbf{F}^{\mathrm{H}}\mathbf{F})$ and $C_u = \tan(\pi \cdot K_u^{-1})$ are introduced for simplicity. To obtain a simpler form, we define matrix/vector $\mathbf{P}$, $\mathbf{z}$, $\{\mathbf{a}_u\}$ and $\{\mathbf{b}_u\}$ as follows:

$$\begin{aligned}\mathbf{P} &= \begin{bmatrix}\mathbf{Q}_{\mathrm{R}} & -\mathbf{Q}_{\mathrm{I}} \\ \mathbf{Q}_{\mathrm{I}} & \mathbf{Q}_{\mathrm{R}}\end{bmatrix} \in \mathbb{R}^{2M\times 2M},\ \ \mathbf{z} = \begin{bmatrix}\mathbf{x}_{\mathrm{R}} \\ \mathbf{x}_{\mathrm{I}}\end{bmatrix} \in \mathbb{R}^{2M}, \\ \mathbf{a}_u^{\mathrm{T}} &= \left[C_u\tilde{\mathbf{h}}_{\mathrm{R},u}^{\mathrm{T}} + \tilde{\mathbf{h}}_{\mathrm{I},u}^{\mathrm{T}}, C_u\tilde{\mathbf{h}}_{\mathrm{I},u}^{\mathrm{T}} - \tilde{\mathbf{h}}_{\mathrm{R},u}^{\mathrm{T}}\right],\ (\forall\, u \in \mathcal{U}), \\ \mathbf{b}_u^{\mathrm{T}} &= \left[C_u\tilde{\mathbf{h}}_{\mathrm{R},u}^{\mathrm{T}} - \tilde{\mathbf{h}}_{\mathrm{I},u}^{\mathrm{T}}, C_u\tilde{\mathbf{h}}_{\mathrm{I},u}^{\mathrm{T}} + \tilde{\mathbf{h}}_{\mathrm{R},u}^{\mathrm{T}}\right],\ (\forall\, u \in \mathcal{U}).\end{aligned}$$

Then, problem (7) can be equivalently expressed as

$$\begin{aligned}\min_{\mathbf{z}}\ & \mathbf{z}^{\mathrm{T}}\mathbf{P}\mathbf{z}/2 \\ \text{s.t.}\ & \mathbf{a}_u^{\mathrm{T}}\mathbf{z} \geq \gamma_u,\ \mathbf{b}_u^{\mathrm{T}}\mathbf{z} \geq \gamma_u,\ (\forall\, u \in \mathcal{U}).\end{aligned} \quad (8)$$

We use dual ascent method to design an iterative algorithm. Let $\boldsymbol{\phi}(\{\lambda_u, \mu_u\}) = \sum_{u=1}^{U}(\lambda_u\mathbf{a}_u + \mu_u\mathbf{b}_u)$. The Lagrange dual problem of problem (8) is given by

$$\begin{aligned}\min_{\{\lambda_u,\mu_u\}}\ & \frac{1}{2}\boldsymbol{\phi}^{\mathrm{T}}(\{\lambda_u,\mu_u\})\mathbf{P}^{-1}\boldsymbol{\phi}(\{\lambda_u,\mu_u\}) - \sum_{u=1}^{U}\gamma_u(\lambda_u+\mu_u) \\ \text{s.t.}\ & \lambda_u \geq 0,\ \mu_u \geq 0,\ (\forall\, u \in \mathcal{U}),\end{aligned} \quad (9)$$

where λ_u and μ_u are dual variables for constraints $\mathbf{a}_u^{\mathrm{T}}\mathbf{z} \geq \gamma_u$ and $\mathbf{b}_u^{\mathrm{T}}\mathbf{z} \geq \gamma_u$, respectively. If $\{\lambda_u^\star, \mu_u^\star\}$ solves problem (9), the primal solution can be recovered via

$$\mathbf{z}^\star = \mathbf{P}^{-1}\boldsymbol{\phi}(\{\lambda_u^\star, \mu_u^\star\}). \quad (10)$$

Since problem (9) is separable, the coordinate ascent method can be utilized. Moreover, each dual sub-problem has a closed-form solution, which is given by

$$\lambda_u \leftarrow \max\left\{0, \lambda_u + \frac{\gamma_u - \mathbf{a}_u^{\mathrm{T}}\mathbf{P}^{-1}\boldsymbol{\phi}(\{\lambda_u,\mu_u\})}{\mathbf{a}_u^{\mathrm{T}}\mathbf{P}^{-1}\mathbf{a}_u}\right\} \quad (11)$$

$$\mu_u \leftarrow \max\left\{0, \mu_u + \frac{\gamma_u - \mathbf{b}_u^{\mathrm{T}}\mathbf{P}^{-1}\boldsymbol{\phi}(\{\lambda_u,\mu_u\})}{\mathbf{b}_u^{\mathrm{T}}\mathbf{P}^{-1}\mathbf{b}_u}\right\}. \quad (12)$$

The derived iterative algorithm is summarized in Algorithm 1.

To design the RM, we further unfold Algorithm 1. Because updating $\{\lambda_u, \mu_u\}$ involves matrix inversion operation $\mathbf{P}^{-1}$, it incurs a high computational complexity. Let $\boldsymbol{\Lambda}$ be the diagonal matrix constructed by extracting the diagonal elements of $\mathbf{P}$. Thanks to the approximate orthogonality of beams in $\mathcal{F}$, $\boldsymbol{\Lambda}$ is dominated for $\mathbf{P}$. By letting $\mathbf{Z} = \mathbf{P} - \boldsymbol{\Lambda}$, $\mathbf{P}$ can be written as $\mathbf{P} = \mathbf{Z} + \boldsymbol{\Lambda}$. Then, $\mathbf{P}^{-1}$ can be approximated by

$$\begin{aligned}(\mathbf{Z}+\boldsymbol{\Lambda})^{-1} =& \boldsymbol{\Lambda}^{-1}\left(\mathbf{I} + \sum_{n=1}^{\infty}(-1)^n\left(\mathbf{Z}\boldsymbol{\Lambda}^{-1}\right)^n\right) \\ \overset{(*)}{\approx}& \boldsymbol{\Lambda}^{-1} - \boldsymbol{\Lambda}^{-1}\mathbf{Z}\boldsymbol{\Lambda}^{-1} + \boldsymbol{\Lambda}^{-1}\mathbf{Z}\boldsymbol{\Lambda}^{-1}\mathbf{Z}\boldsymbol{\Lambda}^{-1},\end{aligned} \quad (13)$$

where $(*)$ is obtained by omitting all n-order $(n \geq 3)$ terms. To reduce possible errors (e.g., due to the approximation), we introduce a trainable matrix parameter $\mathbf{X}$, i.e.,

$$\mathbf{P}^{-1} = \boldsymbol{\Lambda}^{-1} - \boldsymbol{\Lambda}^{-1}\mathbf{Z}\boldsymbol{\Lambda}^{-1} + \boldsymbol{\Lambda}^{-1}\mathbf{Z}\boldsymbol{\Lambda}^{-1}\mathbf{Z}\boldsymbol{\Lambda}^{-1} + \mathbf{X}. \quad (14)$$

Still using the approximate orthogonality of beams in $\mathcal{F}$, $\mathbf{X}$ is set to a band matrix (See Fig. 3), which greatly reduces the scale of learnable parameters and computational complexity.

Algorithm 1: Dual Ascent Algorithm for Problem (8)

1: **input:** matrix $\mathbf{P}$, vectors $\{\mathbf{a}_u\}$ and vectors $\{\mathbf{b}_u\}$
2: **initialize** dual variables $\{\lambda_u \geq 0\}$ and $\{\mu_u \geq 0\}$
3: **repeat**
  (a) **update** $\{\lambda_u\}$ in sequence according to (11)
  (b) **update** $\{\mu_u\}$ in sequence according to (12)
  (c) **check** convergence criterion
4: **until** some convergence criterion is met
5: **output:** primal optimal solution according to (10)

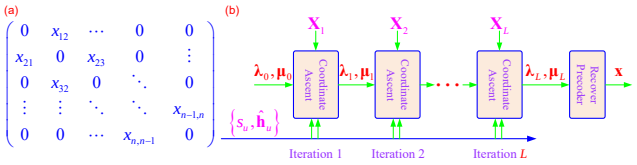

Fig. 3. The architecture/structure of the designed precoding network.

Based on the above discussion, we can unfold Algorithm 1. For clarity, the structure of the designed precoding network (PN), i.e., the unfolded iterative algorithm, is shown in Fig. 3. The PN consists of L layers/iterations, and each layer consists of $2U$ coordinate iteration units whose iterative formulas are given in (11) and (12). The trainable/learnable parameters of PN are $\boldsymbol{\Theta} = \{\mathbf{X}_l \,|\, l = 1, \cdots, L\}$, where $\mathbf{X}_l$ is the learnable matrix parameter within the l-th layer.

B. Training Method

To bring the superiority of the JPR framework into full play, we further tailor an online learning method.

1) Train PN and Optimize $\boldsymbol{\Theta}$: When training PN, $\mathbf{F}$ should be fixed. As a mapping, the PN is denoted by $\mathcal{G}(\cdot, \boldsymbol{\Theta})$. The input of $\mathcal{G}(\cdot)$ includes mCSI $\{\mathbf{h}_u\}$ and transmitted symbols $\{s_u\}$, which are collected into $\mathcal{X}$, i.e., $\mathcal{X} = \{\mathbf{h}_u, s_u \,|\, u \in \mathcal{U}\}$. The predictive output for given input $\mathcal{X}$ is precoder $\mathbf{x}$. Given a training dataset $\mathcal{D}_{\boldsymbol{\Theta}} = \{\mathcal{X}_1, \cdots, \mathcal{X}_n\}$, $\boldsymbol{\Theta}$ is trained as follows.

For each point $\mathcal{X}_i \in \mathcal{D}_{\mathbf{\Theta}}$, the forward propagation (FP) yields a predictive output $\mathcal{G}(\mathcal{X}_i, \mathbf{\Theta})$, and the loss is calculated as

$$L(\mathcal{X}_i) = \|\mathbf{F}\mathcal{G}(\mathcal{X}_i, \mathbf{\Theta})\|^2. \tag{15}$$

With the loss available, $\mathbf{\Theta}$ can be updated via the BP.

2) Train HPPN and Optimize $\mathbf{F}$*:* The network that incorporates both RM (implemented via PN) and PM (corresponding to $\mathbf{F}$) is referred to as hybrid pilot and precoding network (HPPN). As a mapping, HPPN is denoted by $\mathcal{A}(\cdot, \mathbf{F}, \mathbf{\Theta})$. Note that $\mathbf{\Theta}$ is fixed when training HPPN. The input of HPPN is pCSI $\mathcal{H} = \{\bar{\mathbf{h}}_u\}$. The predictive output for $\mathcal{H}$ is still precoder $\mathbf{x}$. With a training dataset $\mathcal{D}_{\mathbf{F}} = \{\mathcal{H}_1, \cdots, \mathcal{H}_n\}$, $\mathbf{F}$ is learned as follows. For each $\mathcal{H}_i \in \mathcal{D}_{\mathbf{F}}$, the FP yields a predictive output $\mathcal{A}(\mathcal{H}_i, \mathbf{F}, \mathbf{\Theta})$. The loss is similarly calculated as

$$L(\mathcal{H}_i, \mathbf{x}_i) = \|\mathbf{F}\mathcal{A}(\mathcal{H}_i, \mathbf{F}, \mathbf{\Theta})\|^2. \tag{16}$$

With the loss available, $\mathbf{F}$ can be updated via the BP.

Algorithm 2: Unified Pilot and Precoding Optimization

1: **input:** K - time-scale of optimizing $\mathbf{F}$, M - number of pilots, F - update frequency of $\mathbf{\Theta}$

2: **initialize** trainable parameters $\mathbf{\Theta}$ and $\mathbf{F}$, empty datasets $\mathcal{D}_{\mathbf{\Theta}} = \emptyset$ and $\mathcal{D}_{\mathbf{F}} = \emptyset$; let $n = 0$

3: **repeat**

(a) **use** $\mathbf{F}$ to transmit signal and estimate mCSI $\{\hat{\mathbf{h}}_u\}$

(b) **design** precoder $\mathbf{x}$ with estimated mCSI via FP

(c) **transmit** symbols with optimized precoder $\mathbf{x}$

(d) **update** $\mathcal{D}_{\mathbf{\Theta}}$ and $\mathbf{D}_{\mathbf{F}}$ with $\{\mathbf{h}_u\}$ and symbols

(e) **update** counter $n \leftarrow n + 1$

(f) **update** $\mathbf{\Theta}$ and $\mathbf{F}$ if conditions are satisfied:

if $n \bmod F = 0$, update $\mathbf{\Theta}$ via BP with $\mathcal{D}_{\mathbf{\Theta}}$

if $n \bmod K = 0$, update $\mathbf{F}$ via BP with $\mathcal{D}_{\mathbf{F}}$

The designed online training method for JPR is summarized in Algorithm 2. In step 1, we determine the system parameters. We initialize the trainable parameters $\mathbf{\Theta}$ and $\mathbf{F}$ and empty the datasets in step 2. In each time-slot, we perform the following operations. In step 3-(a), we use $\mathbf{F}$ to estimate mCSI , based on which the precoder $\mathbf{x}$ can be obtained in step 3-(b). With $\mathbf{x}$ available, we use it to transmit information symbols in step 3-(c). In steps 3-(d) and 3-(e), we update the datasets. Finally, if the conditions are satisfied, $\mathbf{\Theta}$ and $\mathbf{F}$ are updated.

V. Simulation Results

In this section, simulation results are provided to evaluate the proposed algorithms. For comparison, the fully-DNN SLP (DNN-SLP) solution in [15], the fully-digital SLP (FD-SLP) solution of [20], the fully-sweeping SLP (FS-SLP) solution in [3] and eigen-decomposition plus sweeping SLP (EDS-SLP) solution in [20] are chosen as benchmarks to evaluate the proposed JPR-SLP solution. Note that the above solutions use DNN, identity matrix $\mathbf{I}$, DFT matrix and eigenvectors as pilot beams, respectively. Symbol error rate (SER), transmit power, training/feedback overhead and normalized MSE (NMSE) are chosen as performance metrics. Let $\hat{\mathbf{x}}$ (or $\mathbf{x}^\star$) denote predicted (or optimal) precoder. Then, NMSE is defined as

$$\text{NMSE} = 10\log\left(\|\hat{\mathbf{x}} - \mathbf{x}^\star\|^2 / \|\mathbf{x}^\star\|^2\right). \tag{17}$$

Without loss of generality, spatial correlation channel model with uniform linear array is considered [18], [19]. The downlink channel covariance matrix of UE u can be written as

$$\mathbf{R}_u = \int_{\bar{\theta}_u - \Delta_u}^{\bar{\theta}_u + \Delta_u} S_u(\theta)\mathbf{a}(\theta)\mathbf{a}^{\mathrm{H}}(\theta)d\theta, \tag{18}$$

where $S_u(\theta)$ denotes power angular spectrum (PAS) function of $\bar{\mathbf{h}}_u$ and characterizes channel power distribution in the angular domain [18]. $[\bar{\theta}-\Delta, \bar{\theta}+\Delta]$ denotes angle spread (AS) and $\mathbf{a}(\cdot)$ is array response vector. Note that for more general and complex channel models, the developed algorithms can be applied directly. In this section, uniform distribution PAS, i.e., $S(\theta) = 0.5/\Delta\,(\forall\,\theta \in [\bar{\theta} - \Delta, \bar{\theta} + \Delta])$, is adopted. The real mCSI $\mathbf{h}_u$ and estimated mCSI $\hat{\mathbf{h}}_u$ satisfy

$$\mathbf{h}_u = \hat{\mathbf{h}}_u + \Delta\mathbf{h}_u^{\mathrm{G}} + \Delta\mathbf{h}_u^{\mathrm{Q}}, \tag{19}$$

where $\Delta\mathbf{h}_u^{\mathrm{G}}$ and $\Delta\mathbf{h}_u^{\mathrm{Q}}$ denote the Gaussian noise (distributed as $\mathcal{CN}(0, \sigma_{\mathrm{G}}^2\mathbf{I})$) and quantization noise, respectively [20]. The simplest uniform element-wise scalar quantization is used.

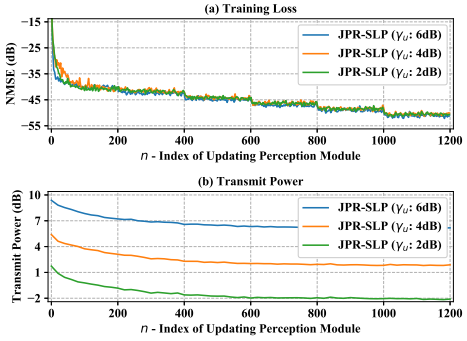

Fig. 4. The learning/convergence performance of JPR-SLP (i.e., Algorithm 2): $M = 15$, $\sigma_{\mathrm{G}}^2 = 0.04$, $K = 50$ and $Q = 8$ (number of quantization bits). The PM module or matrix $\mathbf{F}$ is randomly initialized.

First, we demonstrate the learning/convergence performance of JPR-SLP (i.e., Algorithm 2), as shown in Fig. 4. It is seen that JPR-SLP learns fast and a good NMSE performance can be achieved with only 400 updates (or $400K$ time-slots). The reason for this is that the AU technique is utilized to generate the reasoning network, which, in fact, incorporates much prior knowledge. As a result, less samples are required, i.e., a small sample performance can be achieved. It is also observed that as n (i.e., times that the PM module updates) increases, the required transmit power decreases. The reason for this is that as the quality of the perception matrix $\mathbf{F}$ becomes better and captures more accurate precoding-sensitive statistical information, the quality of the estimated mCSI also becomes better. Therefore, less transmit power is required to achieve the same performance (measured by $\{\gamma_u\}$).

The SER performance of EDS-SLP and JPR-SLP solutions with varying pilot budget is shown in Fig. 5. It is not surprising

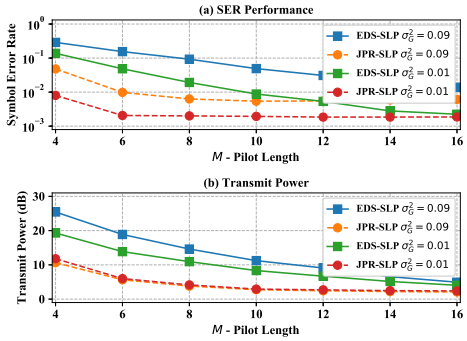

Fig. 5. The SER performance of different algorithms varies with the number of available pilots M: $U = 3$, $N = 64$, $\Delta = 0.09$ (AS) and QPSK.

that JPR-SLP achieves the better performance, in terms of both required transmit power and SER. The reason for this is that the optimization or update of the PM network is under the guide of the RM module, which guarantees that the extracted channel statistical information is needed most by the precoding algorithm. In contrast, EDS-SLP is a heuristic design. As for DNN-SLP, it is completely represented and implemented via DNN, which requires a huge number of training sample and has to be trained offline.

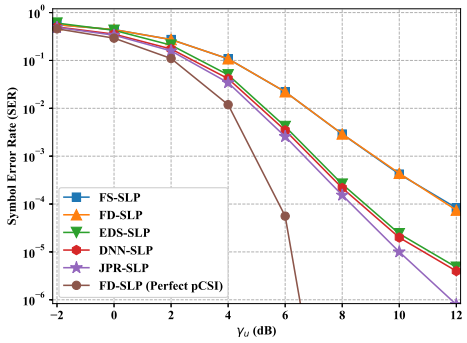

Fig. 6. The SER performance of different algorithms: $N = 64$, $\Delta = 0.09$ (AS), $M = 12$ (EDS-SLP, DNN-SLP and JPR-SLP), $\sigma_G^2 = 0.16$ and QPSK.

TABLE I
TRAINING AND FEEDBACK OVERHEADS (NORMALIZED TO N)

Algorithm	FD-SLP	FS-SLP	EDS-SLP	JPR-SLP	DNN-SLP
Training	1.0	1.0	0.1875	0.1875	0.1875
Feedback	1.0	1.0	0.1875	0.1875	0.1875

The SER performance of different SLP algorithms is shown in Fig. 6. The training and feedback overheads are compared in Table I. It is not surprising that JPR-SLP achieves the best SER performance among all SLP algorithms, with inaccurate pCSI or pCSI. The reason for this is two-fold. On the one hand, important mCSI is sensed and captured by the PM module. On the other hand, unimportant inaccurate mCSI is discarded, which avoids the noise amplification effect. In addition to the good SER performance, another important advantage of JPR-SLP is that the training and feedback overheads of JPR-SLP are much less than those of the other algorithms, which is very appealing for large-scale FDD downlink systems.

VI. CONCLUSION

In this paper we proposed the rCSI-TSP framework, based on which we further proposed an efficient precoding approach. Firstly, we provided the theoretical foundation of rCSI-TSP. Then, we implemented the framework by incorporating PM and RM. In particular, the RM is implemented via AU. Based on rCSI-TSP, we designed an efficient precoding algorithm for the multi-user FDD downlink system.

REFERENCES

[1] F. Rusek, D. Persson, B. K. Lau, E. G. Larsson, T. L. Marzetta, O. Edfors, and F. Tufvesson, "Scaling up MIMO: Opportunities and challenges with very large arrays," *IEEE Signal Process. Mag.*, vol. 30, no. 1, pp. 40–60, 2013.

[2] F. Sohrabi and W. Yu, "Hybrid digital and analog beamforming design for large-scale antenna arrays," *IEEE J. Sel. Topics Signal Process.*, vol. 10, no. 3, pp. 501–513, 2016.

[3] S. He, J. Wang, Y. Huang, B. Ottersten, and W. Hong, "Codebook-based hybrid precoding for millimeter wave multiuser systems," *IEEE Trans. Signal Process.*, vol. 65, no. 20, pp. 5289–5304, Oct 2017.

[4] C. Masouros and E. Alsusa, "Dynamic linear precoding for the exploitation of known interference in MIMO broadcast systems," *IEEE Trans. Wireless Commun.*, vol. 8, no. 3, pp. 1396–1404, 2009.

[5] C. Masouros, "Correlation rotation linear precoding for MIMO broadcast communications," *IEEE Trans. Signal Process.*, vol. 59, no. 1, pp. 252–262, 2011.

[6] C. Masouros and T. Ratnarajah, "Interference as a source of green signal power in cognitive relay assisted co-existing MIMO wireless transmissions," *IEEE Trans. Commun.*, vol. 60, no. 2, pp. 525–536, 2012.

[7] C. Masouros, M. Sellathurai, and T. Ratnarajah, "Vector perturbation based on symbol scaling for limited feedback MISO downlinks," *IEEE Trans. Signal Process.*, vol. 62, no. 3, pp. 562–571, 2014.

[8] A. Adhikary, J. Nam, J. Ahn, and G. Caire, "Joint spatial division and multiplexing - the large-scale array regime," *IEEE Trans. Inf. Theory*, vol. 59, no. 10, pp. 6441–6463, 2013.

[9] A. Liu and V. K. N. Lau, "Two-stage constant-envelope precoding for low-cost massive MIMO systems," *IEEE Trans. Signal Process.*, vol. 64, no. 2, pp. 485–494, 2016.

[10] A. Almradi, M. Matthaiou, and V. F. Fusco, "Two-stage limited feedback hybrid precoding in multiuser MIMO systems," in *2020 IEEE International Conference on Communications (ICC)*, 2020, pp. 1–7.

[11] J. Nam, Y.-J. Ko, and J. Ha, "User grouping of two-stage MU-MIMO precoding for clustered user geometry," *IEEE Commun. Lett.*, vol. 19, no. 8, pp. 1458–1461, 2015.

[12] A. Alkhateeb, G. Leus, and R. Heath, "Limited feedback hybrid precoding for multi-user millimeter wave systems," *IEEE Trans. Wireless Commun.*, vol. 14, no. 11, pp. 6481–6494, Nov 2015.

[13] J. Zhang, Y. Huang, J. Wang, X. You, and C. Masouros, "Intelligent interactive beam training for millimeter wave communications," *IEEE Trans. Wireless Commun.*, vol. 20, no. 3, pp. 2034–2048, 2021.

[14] H. Sun, X. Chen, Q. Shi, M. Hong, X. Fu, and N. D. Sidiropoulos, "Learning to optimize: Training deep neural networks for interference management," *IEEE Trans. Signal Process.*, vol. 66, no. 20, pp. 5438–5453, 2018.

[15] F. Sohrabi, K. M. Attiah, and W. Yu, "Deep learning for distributed channel feedback and multiuser precoding in FDD massive mimo," *IEEE Trans. Wireless Commun.*, vol. 20, no. 7, pp. 4044–4057, 2021.

[16] V. Monga, Y. Li, and Y. C. Eldar, "Algorithm unrolling: Interpretable, efficient deep learning for signal and image processing," *IEEE Signal Process. Mag.*, vol. 38, no. 2, pp. 18–44, 2021.

[17] E. Björnson, J. Hoydis, M. Kountouris, and M. Debbah, "Massive MIMO systems with non-ideal hardware: Energy efficiency, estimation, and capacity limits," *IEEE Trans. Inf. Theory*, vol. 60, no. 11, pp. 7112–7139, 2014.

[18] H. Xie, F. Gao, S. Jin, J. Fang, and Y. Liang, "Channel estimation for TDD/FDD massive MIMO systems with channel covariance computing," *IEEE Trans. Wireless Commun.*, vol. 17, no. 6, pp. 4206–4218, 2018.

[19] Y. Yang, F. Gao, Z. Zhong, B. Ai, and A. Alkhateeb, "Deep transfer learning-based downlink channel prediction for FDD massive mimo systems," *IEEE Trans. Commun.*, vol. 68, no. 12, pp. 7485–7497, 2020.
[20] C. Masouros and G. Zheng, "Exploiting known interference as green signal power for downlink beamforming optimization," *IEEE Trans. Signal Process.*, vol. 63, no. 14, pp. 3628–3640, 2015.
[21] J. Zhang and C. Masouros, "A unified framework for precoding and pilot design for fdd symbol-level precoding," *IEEE Trans. Wireless Commun.*, pp. 1–1, 2021.